Scientific Research Publishing

International Journal of Modern Nonlinear Theory and Application, 2023, 12, 30-54
https://www.scirp.org/journal/ijmnta
ISSN Online: 2167-9487
ISSN Print: 2167-9479

Classification to Stationary Process of Tidal Motion Observed at the Time of Kuroshio's Meandering

Kenta Kirimoto

Department of Creative Engineering, National Institute of Technology Kitakyushu College, Fukuoka, Japan
Email: kirimoto@kct.ac.jp

How to cite this paper: Kirimoto, K. (2023) Classification to Stationary Process of Tidal Motion Observed at the Time of Kuroshio's Meandering. *International Journal of Modern Nonlinear Theory and Application*, **12**, 30-54.
https://doi.org/10.4236/ijmnta.2023.121003

Received: February 23, 2023
Accepted: March 28, 2023
Published: March 31, 2023

Abstract

The tide level displays information about the state of the sea current and the tidal motion. The tide level of the southern coast of Japan Island is affected strongly by Kuroshio Current flowing in the western part of North Pacific Ocean. When Kuroshio takes the straight path and flow along the Japan Islands, the tide level increases, and it is calculated from two tide level data observed at Kushimoto and Uragami in the southern part of Kii Peninsula. In contrast, the tide level decreases at the time when Kuroshio leaves from the Japan Islands. In this paper, the hourly tidal data are analyzed using the Autocorrelation Function (ACF) and the Mutual Information (MI) and the phase trajectories at first. We classify the results into 5 types of tidal motion. Each categorized type is investigated and characterized precisely using the mean tide level and the unit root test (ADF test) next. The frequency of the type having unstable tidal motion increases when the Kuroshio Current is non-meandering or in a transition state or the tide level is high, and the type shows a non-stationary process. On the other hand, when the Kuroshio Current meanders, the tidal motion tends to take a periodical and stable state and the motion is a stationary process. Though it is not frequent, we also discover a type of stationary and irregular tidal motion.

Keywords

Kuroshio Current, Tide Level, Autocorrelation Function, Mutual Information, Unit Root Test, Phase Trajectories, Stationary Process

1. Introduction

Kuroshio Current flows from west to east in the southern part of the Japan Islands, and it is the most famous warm current on the west coast of North Pacific

Ocean. The width of Kuroshio is about 100 km long, and the drift speed is 2 to 4 knots [1] [2]. Kuroshio affects not only the ship navigation route, but also the climate of the southern coast of Japan due to its heat energy carried from Equator [3] [4] [5] [6]. In addition, Kuroshio gives a strong influence on the reproduction amount of fishery resources and the visit to a coastal area [7] [8]. The most popular ways to estimate the Kuroshio's route are the monitoring of its surface temperature received by satellite remote sensors at the present. In the latest research, Kuroshio's route can be estimated by measuring the rise of sea level because warm sea current lifts the sea level [9]. The sea current data can also be observed directly using equipment such as ocean buoys or ocean research ships [10]. Japan Coast Guard analyzes a wide range of data and determines Kuroshio's route.

Kuroshio's route continuously changes, and its flow path takes three typical patterns which are called straight path, small meandering path and large meandering path [11]. The straight path is one of the routes Kuroshio flows near the coast of Kii Peninsula. When the Kuroshio Current takes a straight path, the tide level rises because the coast blocks the Kuroshio's flow. Therefore, serious attention should be paid to the strong current and the high tide. Japan Coast Guard announces prediction of the tide level and flow path to warn the people who enjoy marine leisure or work on the ship. A small meandering path is defined as the Kuroshio meanders in the east of Kii Peninsula. A large meandering path is defined as the Kuroshio meanders in offshore of Kii Peninsula. The Kuroshio Current is well known to affect the tide level and tidal motion, so the observation of the tide level is the most common method of Kuroshio monitoring. When Kuroshio largely meanders on the Japanese southern coast, the tide level is lowered and the meandering situation will continue and the route won't recover for a few years. Today, the tide level is observed at more than 150 measurement points of tide gauge stations located in Japan and about 20 tide gauge stations are placed at Kuroshio's route. A huge amount of data can be used for this research and opened to the public online system [12]. The study on the meandering and path of the Kuroshio Current has been performed energetically until now by many researchers. Nakano *et al.* insist that Kuroshio vortex which appears at the side of Kuroshio's mainstream often deeply affects the change of Kuroshio path, particularly when predicting the flow path [13]. Large meandering arises after a large Kuroshio vortex occurs at the southern part of Kuroshio's mainstream. Once large meandering arises, another vortex appears between Kii Peninsula and Kuroshio Current. Though ocean current and vortex are chaotic phenomena and it is difficult to predict Kuroshio's path, Kuroshio keeps meandering while the vortex continues.

The development of time series analysis is remarkable recently. Although the application was mainly used for science and technology in the past, they are also used for finance and economy fields today. The augmented Dickey-Fuller test proposed by Graham *et al.* in 1996 is a famous new method of stock analysis, which inspects the null hypothesis that a unit root exists in a time series sample.

When the process doesn't have a unit root, it is a stationary process and exhibits a mean-reverting. As we stated above, the tide level is affected by the Kuroshio Current. Weekly and monthly predictions of Kuroshio path and tidal motion which will be fundamental technologies of our new society will be highly demanded for weather forecast, fishing industry and marine leisure.

The purpose of this paper is to study the social use of the open data application using the time series analysis, and contribute to the physical oceanography which describes the complex fluid motion. According to the previous study, the tidal motion was discussed using the time-frequency analysis of tidal data such as Fourier transform and wavelet transform [14] [15]. When comparing the results of analysis at the time of Kuroshio's meandering and non-meandering, we are able to see the difference in the power spectrum of specific frequencies. However, the time-frequency analysis has a weak point on the signals with the trend. Moreover, the analysis of signals with randomness shows the elevation of the background spectrum. This causes a drop in the SN ratio in the notable spectrum. In this paper, we characterize the tide level and tidal motion affected by Kuroshio Current using a combination of Autocorrelation Function (ACF), Mutual Information (MI), unit root test (ADF test) and phase trajectories. Collecting data on hourly tide levels and analyzing them need to discover the correlation between Kuroshio Current and tidal motion. The characterization of tidal motion is the first step and there will be a possibility to be created new businesses using this work in the future.

2. Time Series Data and Analyzing Methods

2.1. Tidal Data

Tide level is originally composed of the astronomical tide and the meteorological tide. The astronomical tide is a rising and falling motion of seawater caused by the tidal force working between the sun and the earth or between the moon and the earth. On the other hands, the meteorological tide is a fluctuation caused by a meteorological disturbance such as air pressure, temperature, wind, and so on. Therefore, many researchers have paid attention to both the astronomical tide and the meteorological tide when they discuss the tidal data of Kuroshio [16]. Most of the researchers have performed following processing such as the moving average of tide level and/or tide killer filter to remove the influence of the astronomical tide [17]. Moreover, one of the common methods to remove meteorological tide is a correction function of air presser and tide level. However, we want to discover the easy analyzing methods which needn't the pre-process that removes the meteorological tide such as moving average. In fact, the meteorological factors affect the tide level, but we do not correct the tide level data in terms of the influence of wind direction, wind velocity, atmospheric pressure in this paper. The influence of the prevailing wind, the seasonal wind, the change of atmospheric pressure when a low pressure comes into our research area are not a serious problem to the results and discussion in this paper. The reason is that

these influences are steady or temporary for the results in order to perform the analysis on one-month basis.

Figure 1(a) shows typical flow paths of Kuroshio Current. The flow paths of Kuroshio are classified into three typical patterns that are called straight Path (I), small meandering Path (II) and large meandering Path (III) [11] [18]. Figure 1(b) shows the locations of tide station Kushimoto and Uragami in the southern part of Kii peninsula. The data from these tide stations receive large influence on Kuroshio's current when it takes straight Path (I) and small meandering Path (II). On the other hand, the effect of Kuroshio's current becomes smaller when it takes large meandering Path (III). Therefore, these stations, Kushimoto and Uragami, in Kii Peninsula are the most important stations for monitoring Kuroshio. We analyze tidal data measured in these two places above because so. However, these two data contain the astronomical effect and to remove the astronomical effect is the biggest problem in this paper. Therefore, we analyze the tide level difference between Kushimoto and Uragami; to calculate the difference we have to subtract Uragami's data from Kushimoto's.

Table 1 shows the terms of Kuroshio meanders occurred 6 times after 1975. The latest Kuroshio meander has started since August 2017 and been continuing more than 5 years. We obtain hourly tidal data from J-DOSS (the Japan Ocean-graphic Data Center-Data On-line Service System) [19]. We analyze tidal data of Kuroshio meander based on these two different periods, one is 2004-2005 and the other is 2017-2020.

Figure 2 shows the processing procedure from the data acquisition to the analysis of tidal data. It is necessary to download Kushimoto and Uragami tidal data after selecting the year of observation and the place. One text file contains yearly tidal data. This file consists of its gauging station number, date and 24 tidal data per one recode that is 26 columns and 365 rows. Serialized hourly data

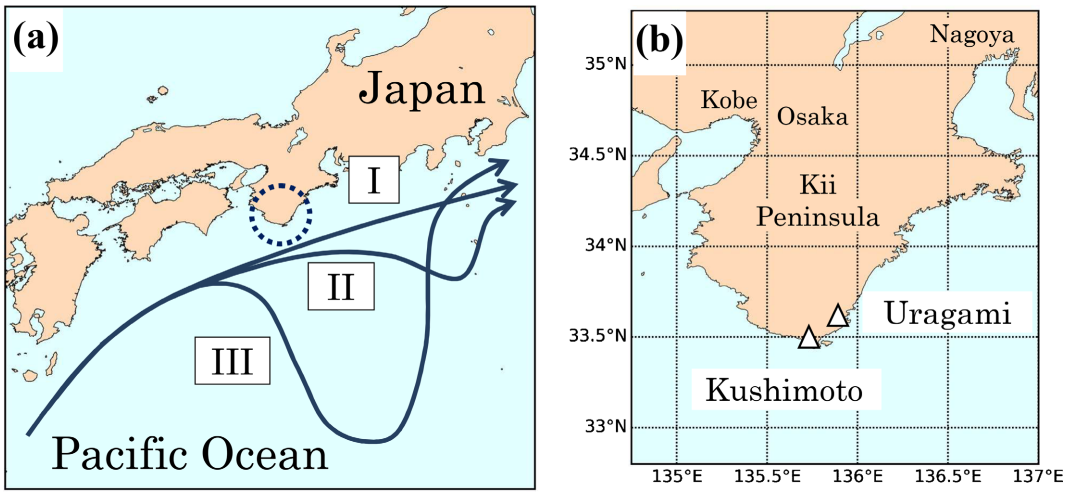

Figure 1. Typical flow paths of Kuroshio Current and location of tide stations in the southern part of Kii Peninsula. (a) Three typical flow paths of Kuroshio Current, Route I is a straight path, Route II is a small meandering path, Route III is a large meandering path. (b) The location of tide stations in the southern part of Kii Peninsula. We use tide level data observed at Kushimoto tide station and Uragami tide station in this paper.

Table 1. Periods on meandering Kuroshio Current after 1975.

Beginning of meandering	Ending of meandering	Duration time
Aug. 1975	Mar. 1980	4 years and 8 months
Nov. 1981	May 1984	2 years and 7 months
Dec. 1986	Jul. 1988	1 year and 8 months
Dec. 1989	Dec. 1990	1 year and 1 month
Jul. 2004	Aug. 2005	1 year and 2 months
Aug. 2017	Continuing at Dec. 2022	5years and 5 months at Dec. 2022

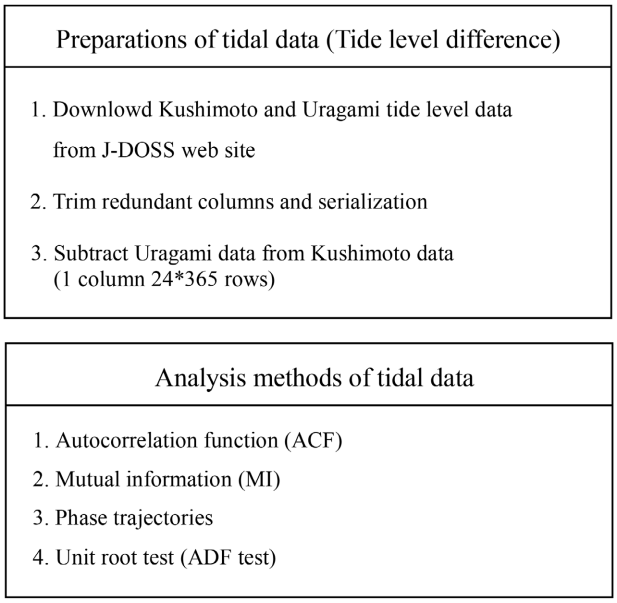

Figure 2. The preparations of tidal data and the analysis methods.

are made by concatenation of all data after removing gauging station number and date column. We make the hourly differential data between Kushimoto and Uragami by the subtraction of Uragami's tide from Kushimoto's tide.

2.2. Autocorrelation Function (ACF)

Discrete time autocorrelation function is a basic method for the time series analysis and is defined by

$$\mathrm{ACF}(lag) = \frac{\sum_{i=0}^{n-lag-1}\{y(i)-\bar{y}\}\{y(i+lag)-\bar{y}\}}{\sum_{i=0}^{n-lag-1}\{y(i)-\bar{y}\}^2}, \quad (1)$$

where $y(i)$ is a time series data, $\bar{y}$ is the mean of $y(i)$, n is the data length, the lag is a time shift index, i is the time index. $\sum_{i=0}^{n-lag-1}\{y(i)-\bar{y}\}^2$ is used for the normalization of ACF, so that ACF(0) = 1. Because ACF is normalized, the value 1 of ACF is given when the signal with a delayed copy of itself completely matches, and the value −1 of ACF is given when the signal has inversion of positive and

negative. ACF is also a commonly used tool for checking randomness in a data set. If it is random, such ACF should be near zero for any and all time lags.

2.3. Mutual Information (MI)

The mutual information of two jointly discrete random variables X and Y is calculated as a double sum,

$$I(X;Y) = \sum_{y\in Y}\sum_{x\in X} p(x,y)\log_2 \frac{p(x,y)}{p(x)\,p(y)}, \tag{2}$$

where $p(x,y)$ is the joint probability mass function of X and Y, and $p(x)$ and $p(y)$ are the marginal probability mass functions of X and Y respectively [20] [21] [22]. The $p(x,y)$ is estimated from a 2D scatterplot of time series data $y(i)$ vs $y(i+lag)$. The $p(x)$ and $p(y)$ mean the probability mass functions from a fixed width histogram of tidal data $y(i)$ and $y(i+lag)$ in this study. MI means the interdependence between two signals. When MI equals 0, it means there is no interdependence and correlation between two signals. Both ACF and MI are used for the reference value which means the similarity between $y(i)$ and $y(i+lag)$ with time lag. These analyses have important role when the phase trajectories are drawn. The lag of the trajectories is selected at the point where ACF intersects an axis first or MI has local minimum first.

2.4. Unit Root Test: Augmented Dicky-Fuller Test (ADF Test)

The Dickey-Fuller test is testing a unit root which is present if $\varphi = 1$ in an autoregressive time series model as followed

$$y(i) = \alpha + \beta i + \varphi y(i-1) + e(i), \tag{3}$$

where $y(i)$ is a time series data, i is the time index, $e(i)$ is a residual error assumed to be white noise, α, β, φ is a regression constant for each. This model would be non-stationary in case of unit root. Equation (3) is written as

$$\Delta y(i) = y(i) - y(i-1) = \alpha + \beta i + \gamma y(i-1) + e(i), \tag{4}$$

where Δ is the first difference operator, γ is a constant defined by $\varphi - 1$. This linear regression model can be used for testing a unit root with constant and deterministic time trend equivalent to testing $\gamma = 0$, namely $y(i)$ is a random walk process. If not and $-1 < 1 + \gamma < 1$, then $y(i)$ would be a stationary process. The Dickey-Fuller test can be replaced by the Augmented Dick-Fuller test which contains higher-order autoregressive process with $\Delta y(i-p)$ in the model, as below,

$$\begin{aligned}\Delta y(i) = {} & \alpha + \beta i + \gamma y(i-1) + \delta_1 \Delta y(i-1) + \delta_2 \Delta y(i-2) + \cdots \\ & + \delta_{lag} \Delta y(i-lag) + e(i).\end{aligned} \tag{5}$$

To make decision of this test, we take the null hypothesis whose data are non-stationary process. To reject the null hypothesis for these tests, the p-value less than 5% is required. Time series data are examined precisely by the numerical methods; unit root test of Augmented Dicky-Fuller [23] [24] [25]. The maxlag

can be estimated as $\text{floor}\left[\left(\text{maximum data length}-1\right)^{\frac{1}{3}}\right]$. In this paper, the maximum data length is 24 hours * 31 days = 744, and the number of maximum time lag is restricted up to 9.

2.5. Analysis of Simulation Data

Three kinds of time series which are known as random model, chaos model and tide-harmonics model are analyzed in this section. First, we apply a white noise signal as random model. This random model $y_1(i)$ is uniformly distributed in the interval [−10, 10], where i is in hour. Second, we analyze a famous chaos system which is called Rössler model. The defining equations are

$$\begin{cases} \dfrac{\mathrm{d}X}{\mathrm{d}t} = -Y - Z \\ \dfrac{\mathrm{d}Y}{\mathrm{d}t} = X + aY \\ \dfrac{\mathrm{d}Z}{\mathrm{d}t} = b + XZ - cZ \end{cases}$$

with $(a,b,c) = (0.2, 0.2, 7.1)$ and $(X(0), Y(0), Z(0)) = (4, 4, 1)$. Rössler model is calculated by the fourth order of Runge-Kutta method, where the time step $\mathrm{d}t = 0.1$. We use the time series of chaos model as $y_2(i) = X(4*i)$ on above equation. Finally, we apply a simple tide-harmonics model. The time series $Y(i)$ with N harmonic constituents is defined as

$$Y(i) = \sum_{n=1}^{N} \cos\left(\frac{\pi}{180}\omega_n i\right),$$

where ω_n is the angular frequency of the nth component in degree per hour. For example, the speed of principal lunar semi-diurnal (twice daily) constituent, typically called M_2 is 28.98 degrees per hour, since the component repeats every 12.421 hours. We also need to consider the tides due to the sun. The solar semi-diurnal component, denoted by S_2 is 30 degrees per hour with a period of 12 hours. The principal lunar diurnal constituents O_1 and K_1 is 13.94, 15.04 degrees per hour, respectively. We apply a tide model with four components (N = 4) and analyze two data series $y_3(i) = 5*Y(i)$ and $y_4(i) = 5*Y(i+2000)$ with time lag. **Figure 3** shows random data, chaos data and two tide-harmonics data. The ACF, MI with time lag and the phase trajectories are showed in **Figure 4** for each data. The analysis of random data shows no correlation between each data in ACF of **Figure 4(a)**. The analysis of MI and the phase trajectories in **Figure 4(a)** also shows the independency between each data [26]. On the other hand, a periodic characteristic in the chaos model and tide-harmonics model is displayed from the periodic features of results in **Figures 4(b)-(d)**. Apparently, the chaos model $y_2(i)$ is similar to tide model $y_4(i)$ in **Figure 3**. However, the analysis of ACF and MI in **Figure 4** shows $y_3(i)$ and $y_4(i)$ complete match which means they are belong to the same system.

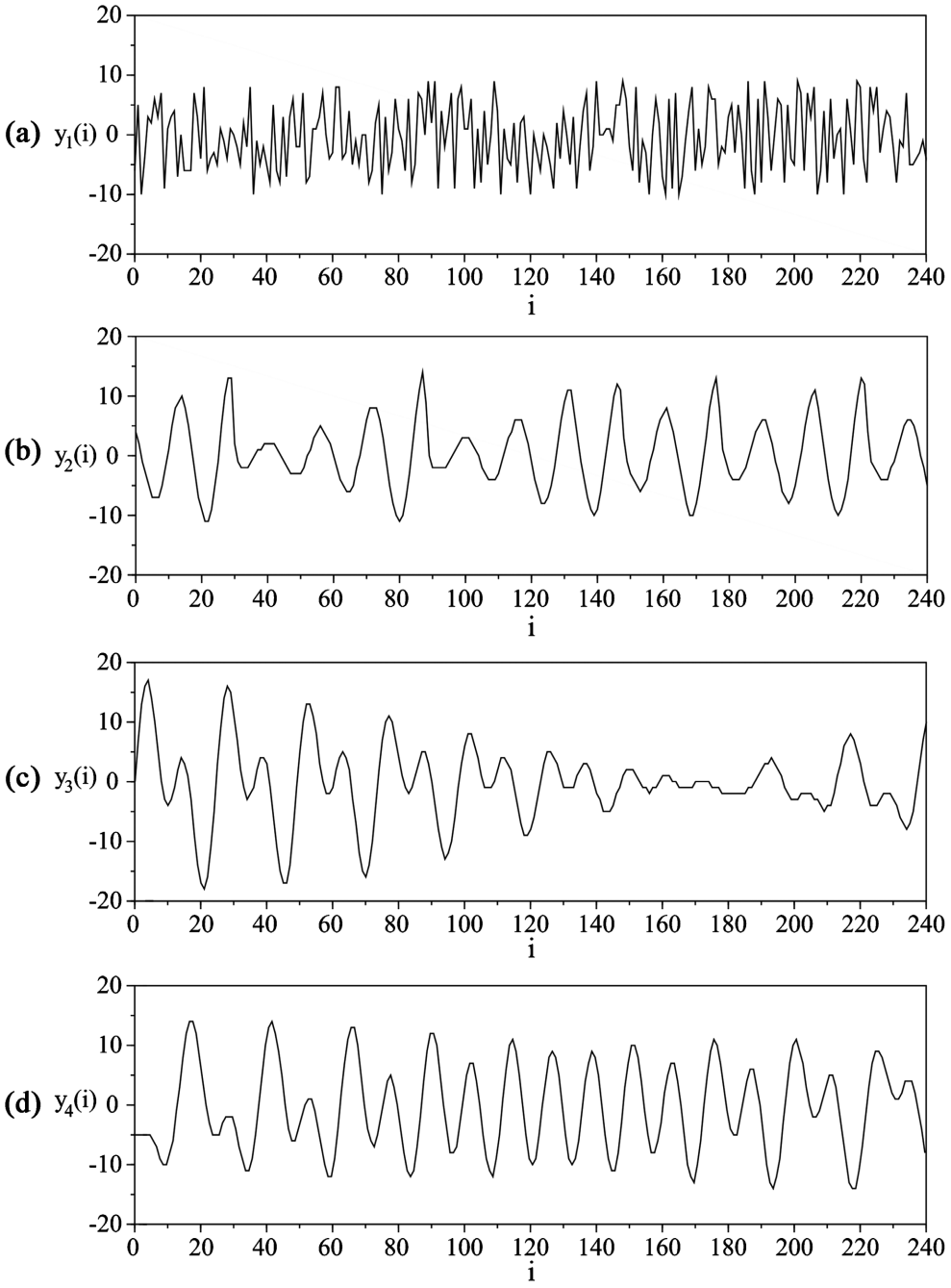

Figure 3. Time series model, (a) random data, (b) chaos data, (c) tide-harmonics data and (d) tide-harmonics data with a time lag.

3. Results and Discussion

Hourly tide level difference data (tidal data) for every month are analyzed in this paper. To remove the astronomical effect, we analyze the tide level difference between Kushimoto and Uragami. The tidal data are calculated by to subtract Uragami's data from Kushimoto's data. Figure 5 shows the tidal data in 2004, 2005, from 2017 to 2020. Kuroshio took the meandering paths for 13 months from July 2004 to August 2005. Moreover, Kuroshio is taking the meandering

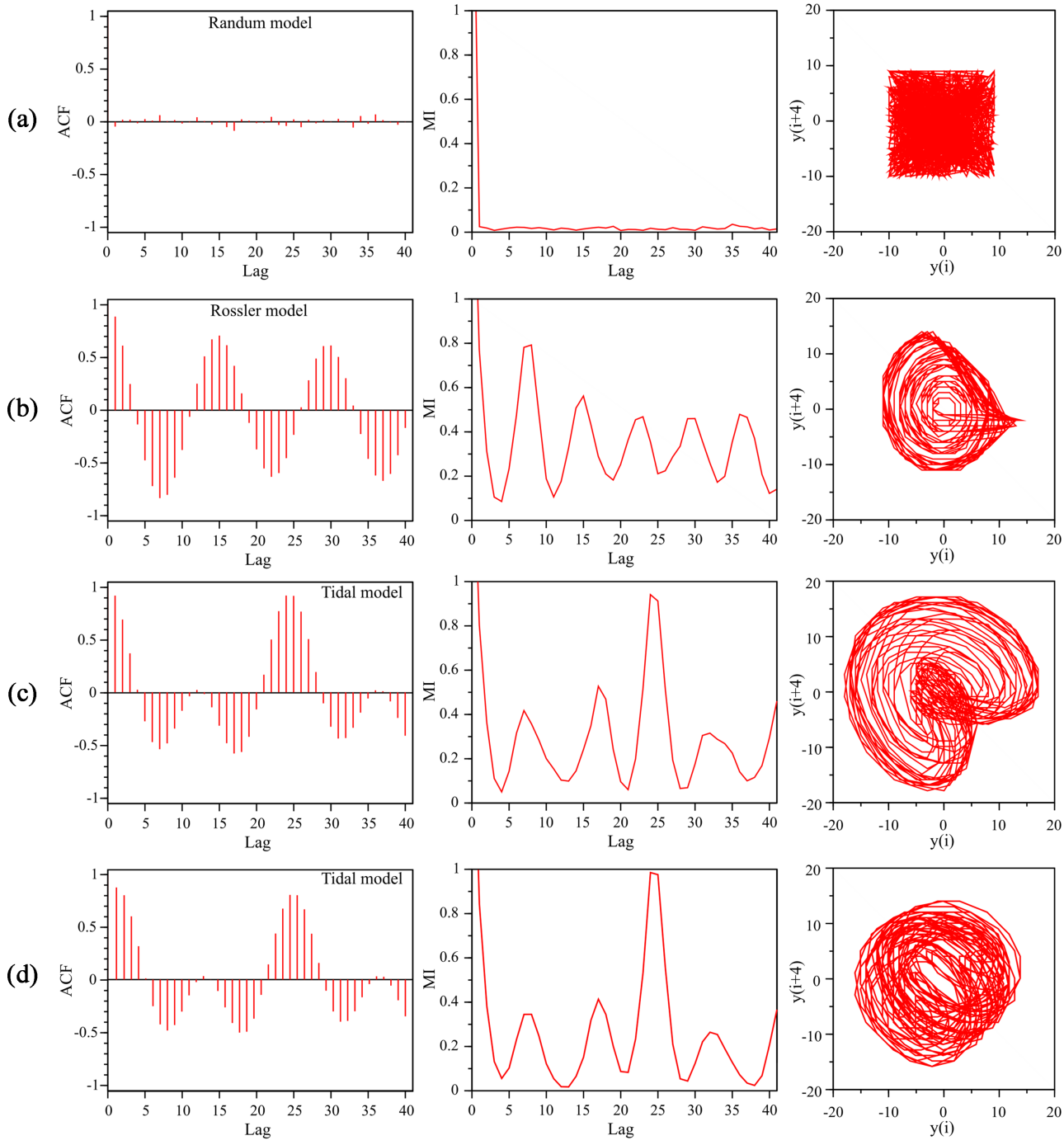

Figure 4. ACF, MI and the phase trajectories of random data, chaos data, tide-harmonics data and tide-harmonics data with a time lag. We use the time lag of 4 hours in the phase trajectories.

paths more than 5 years since August 2017 at December 2022. As shown in **Figure 5**, the tidal data always have some fluctuation. But the tidal data shows up and down trends of fluctuation with the period of few weeks during the non-meandering state. In consequence, we expect to find that tide level of Kushimoto and Uragami is unstable intuitively. Contrariwise, the tidal data are taking low levels in the meandering state. These phenomena are caused by the

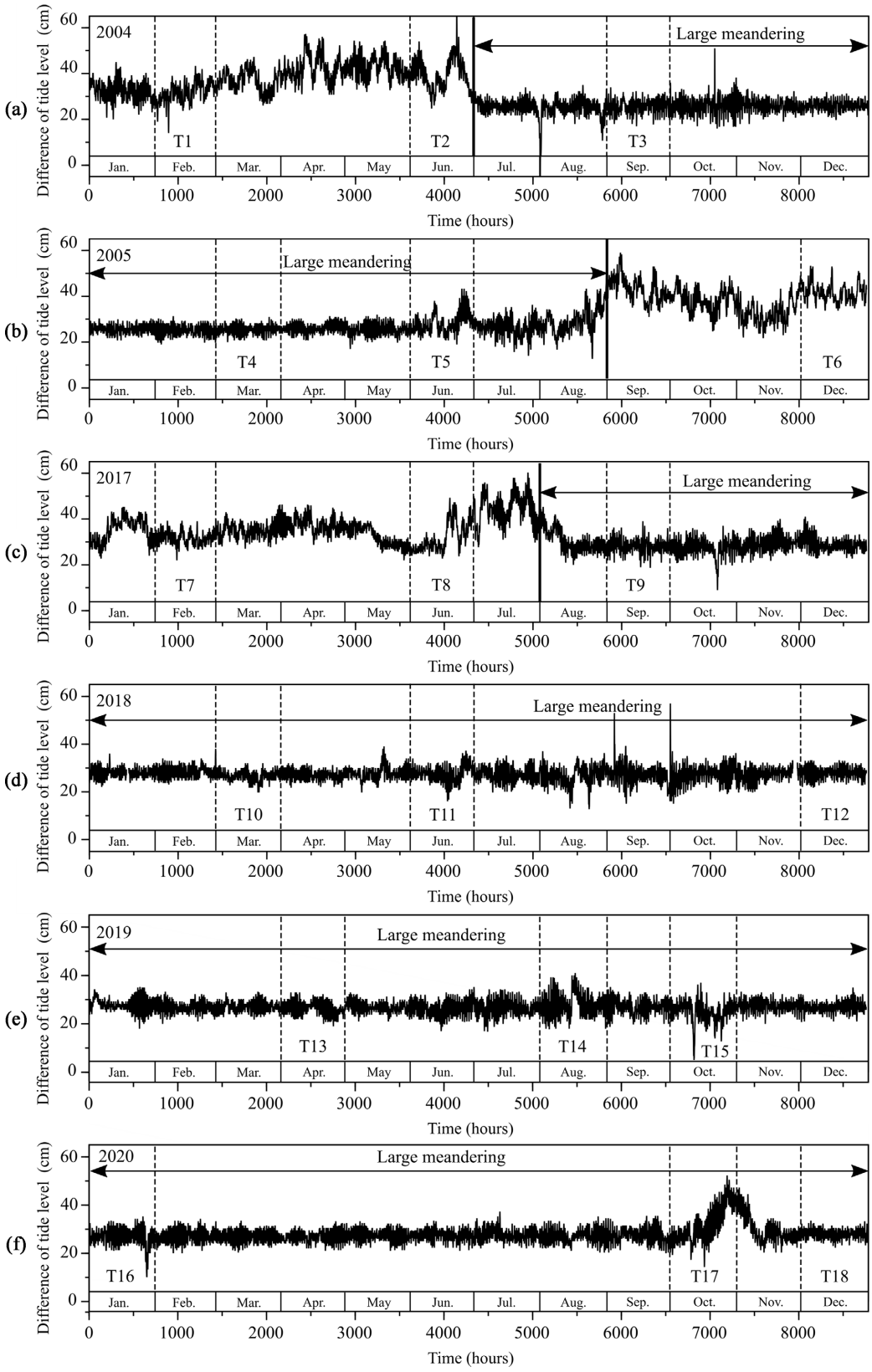

Figure 5. Difference of tide level between Kushimoto and Uragami. Large meandering state started on July 2004, ended on August 2005. Large meandering state started on August 2017 again. T1, T2 and from T6 to T8 are in the non-meandering state. T3, T4, T5 and from T9 to T18 are in the meandering states.

flow field of Kuroshio's flux. The notations from T1 to T18 in Figure 5 show the typical data which we will discuss after.

Figure 6 shows the monthly tidal data which is T2, T4, T6 and T11 shown in Figure 5, respectively. T2 waves up and down most of the time, however, it moves slightly wide some time in Figure 5. Moreover, T2 has uptrend and downtrend a few times within a month. It is difficult to predict tendency of these fluctuations on a long-term basis. Therefore, tidal motion of Type T2 is unstable. T4 continues to take periodical and small fluctuation and the uptrend and

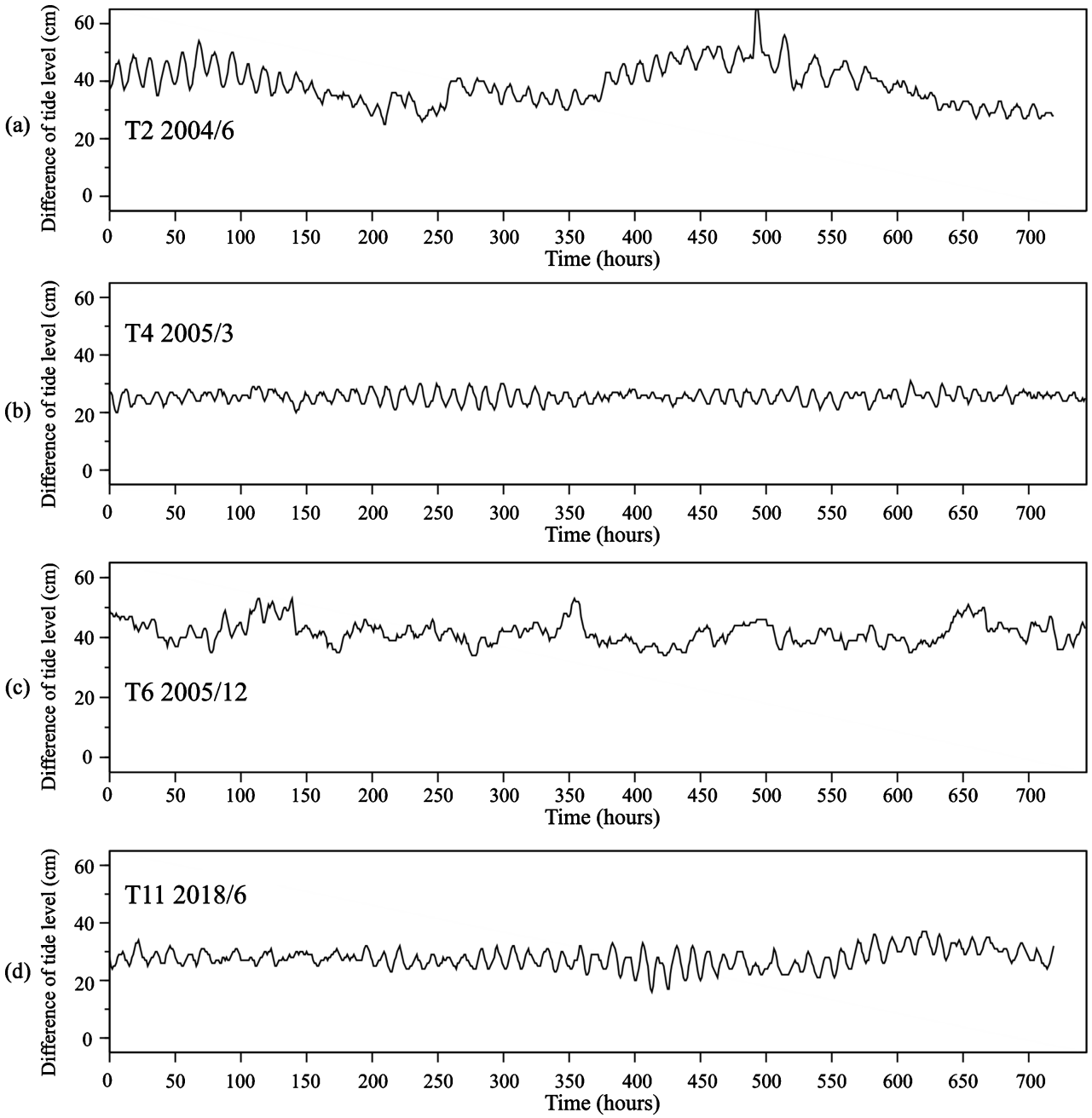

Figure 6. Tide level difference between Kushimoto and Uragami under the meandering state and non-meandering state for a month. T2, T6 and T11 data are non-meandering state. T4 data is meandering state.

downtrend movement cannot be seen over a month, so Type T4 is stationary and stable. The fluctuation of Type T6 is considerably different from T2 and T4. It seems like irregular movement. T11 waves as the same as T2. The uptrend and downtrend are smaller than T2.

Figure 7 shows the ACF, MI and the phase trajectories of tidal data in Figure 6. The horizontal axis in the ACF and MI function are the time lag for each. ACF of T2 is taking a positive value and it fluctuates up and down periodically and

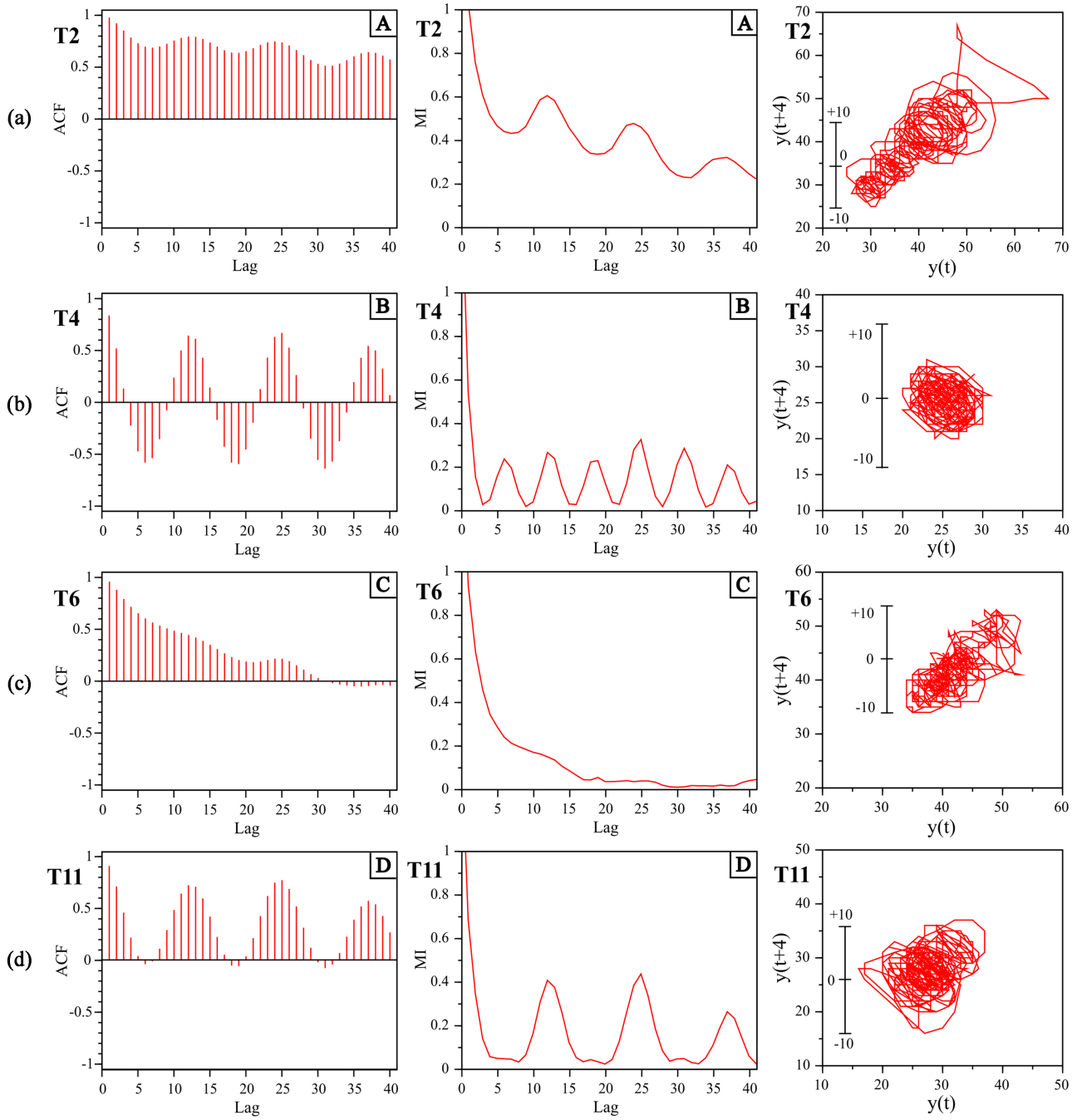

Figure 7. ACF, MI and the phase trajectories of tidal data in Figure 6. T2, T6 and T11 data are in the non-meandering state. T4 data is in the meandering states.

the trend decrease gradually. MI of T2 also fluctuates which period is more than 10 hours long and MI decreases with long time. The phase trajectories of T2 have over 20 cm in size. ACF of T4 fluctuates up and down periodically around 0. ACF has positive and negative value. MI of T4 marks first minimum point within 5 hours and fluctuates up and down until long time lag. The trajectories have a round shape and are relatively small compare to other. It seems the tide keeps a stable state. ACF of T6 is different type compared to others, and the fluctuation of ACF is restrained in comparison with other types and the trend decreases and approaches 0. MI of T6 gradually approaches 0 and finally stays close to 0. The trajectories of T6 are shaped in complicate and intertangle with each other. The minimal points in ACF of T11 can have negative value and it fractures up and down periodically, but ACF is frequently above 0. The fluctuation period of MI is more than 10 hours long. The trajectories of this type make a somewhat round shape. But the tidal motion seems an unstable situation.

From the results above, we reconsider the individual characteristic classification of five different tidal motions based on ACF and MI. **Figure 8** shows ACF, MI and phase trajectories classified Type A. ACF of Type A has positive value and doesn't have negative value. ACF peaks every 12 hours and decreases little by little as time increases. MI also decreases while repeating the strength and weakness as time increases.

Type B is shown in **Figure 9**. ACF of Type B has positive and negative value periodically. Peak of MI appears every 6 hours and each peak is clear. The first minimum appears in MI around 4 hours in time lag and is depressed to the level that is almost 0 with less than 0.03, for example.

Type C is shown in **Figure 10**. ACF of Type C has positive value at first and decrease as time increases. The change of the strength and weakness such as ACF of Type A cannot be seen and it shows considerably gentle curve. When time lag is over 15 hours, ACF becomes apparently small and is closed to 0 and when time lag becomes more than 30 hours, it even has negative value. MI of Type C decreases without waving up and down as time increase. MI of Type C shows less than 0.2 after 15 hours in time lag and keeps low values. When we see **Figure 6(c)** and **Figure 7(c)**, Type C represents a characteristic of an irregularity and the aperiodicity of data.

Type D is shown in **Figure 11**. ACF of Type D has first minimum point after 6 hours. The first maximum point appears after 12 hours and keeps appearing every 12 hours. The fluctuation of MI continues over 40 hours long. The bottom of MI comes after 6 hours and 18 hours. The peak of MI appears after 12 hours and 24 hours same as ACF.

Type E is shown in **Figure 12**. Type E is defined as residual data type, and it doesn't belong to described above. For example, when ACF takes positive values and negative values asymmetrically, we classify it as Type E. MI of Type E has some peaks every 6 hours similar to Type B, but the tidal data are classified into Type E when the height of each peak are obviously different. In the other case,

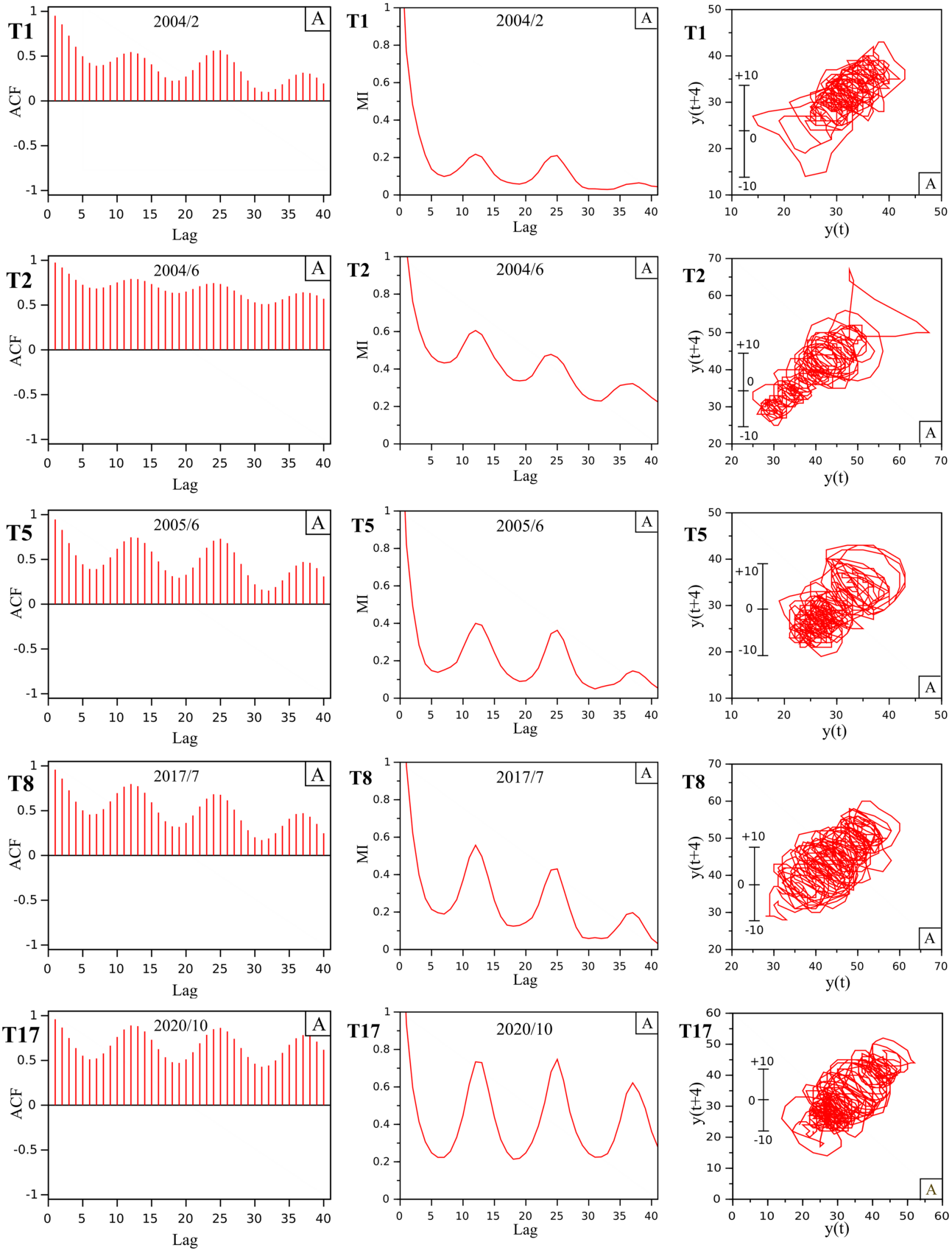

Figure 8. ACF, MI and the phase trajectories of tidal data classified Type A.

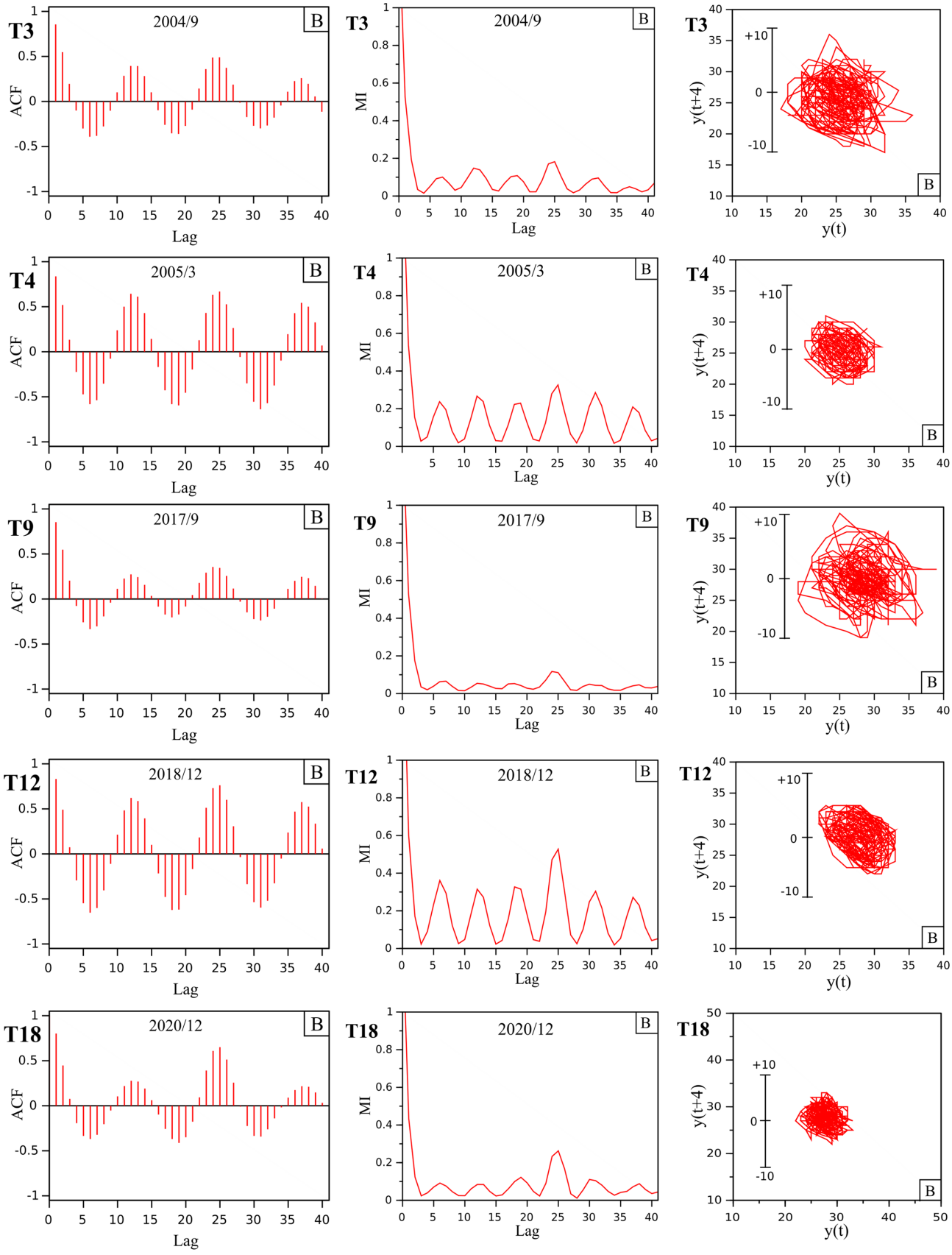

Figure 9. ACF, MI and the phase trajectories of tidal data named Type B.

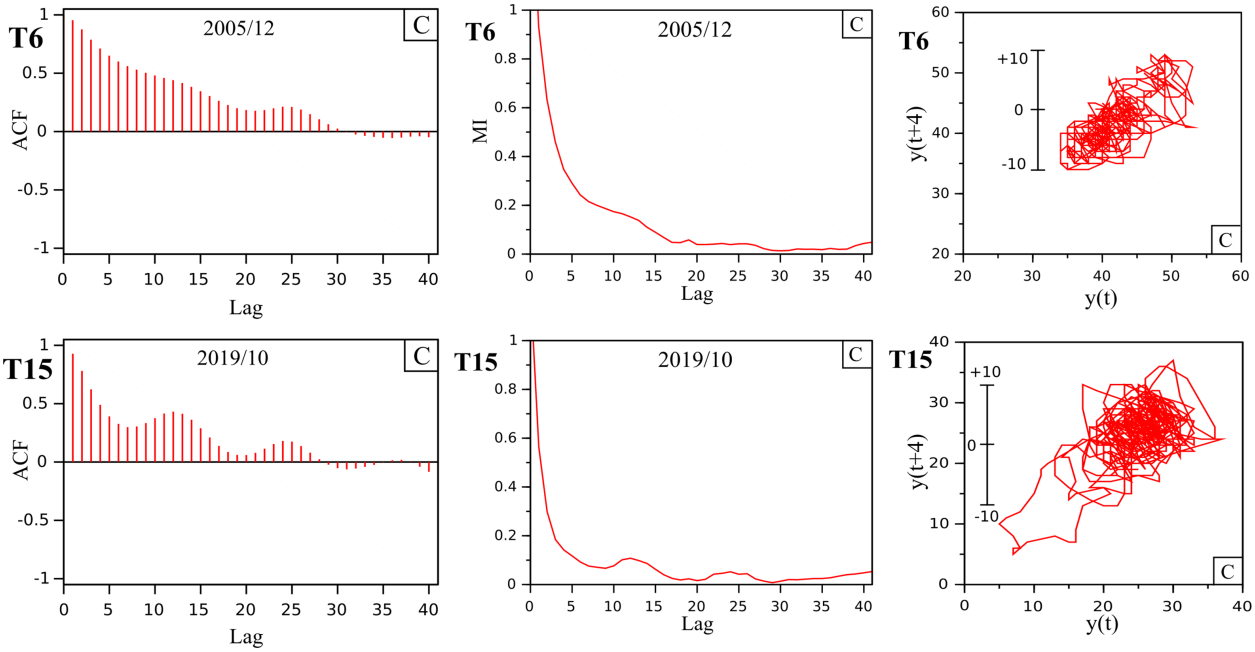

Figure 10. ACF, MI and the phase trajectories of tidal data named Type C.

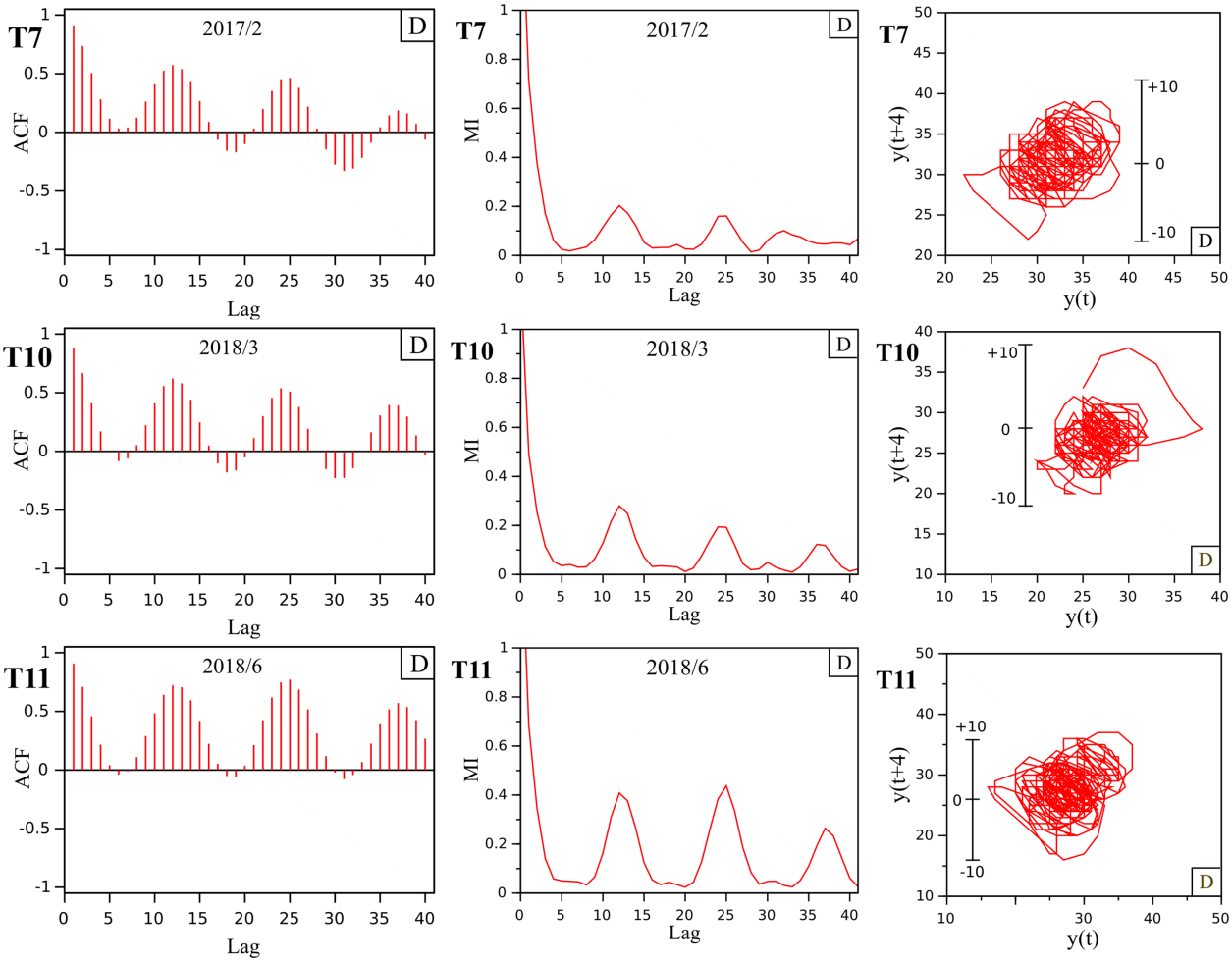

Figure 11. ACF, MI and the phase trajectories of tidal data named Type D.

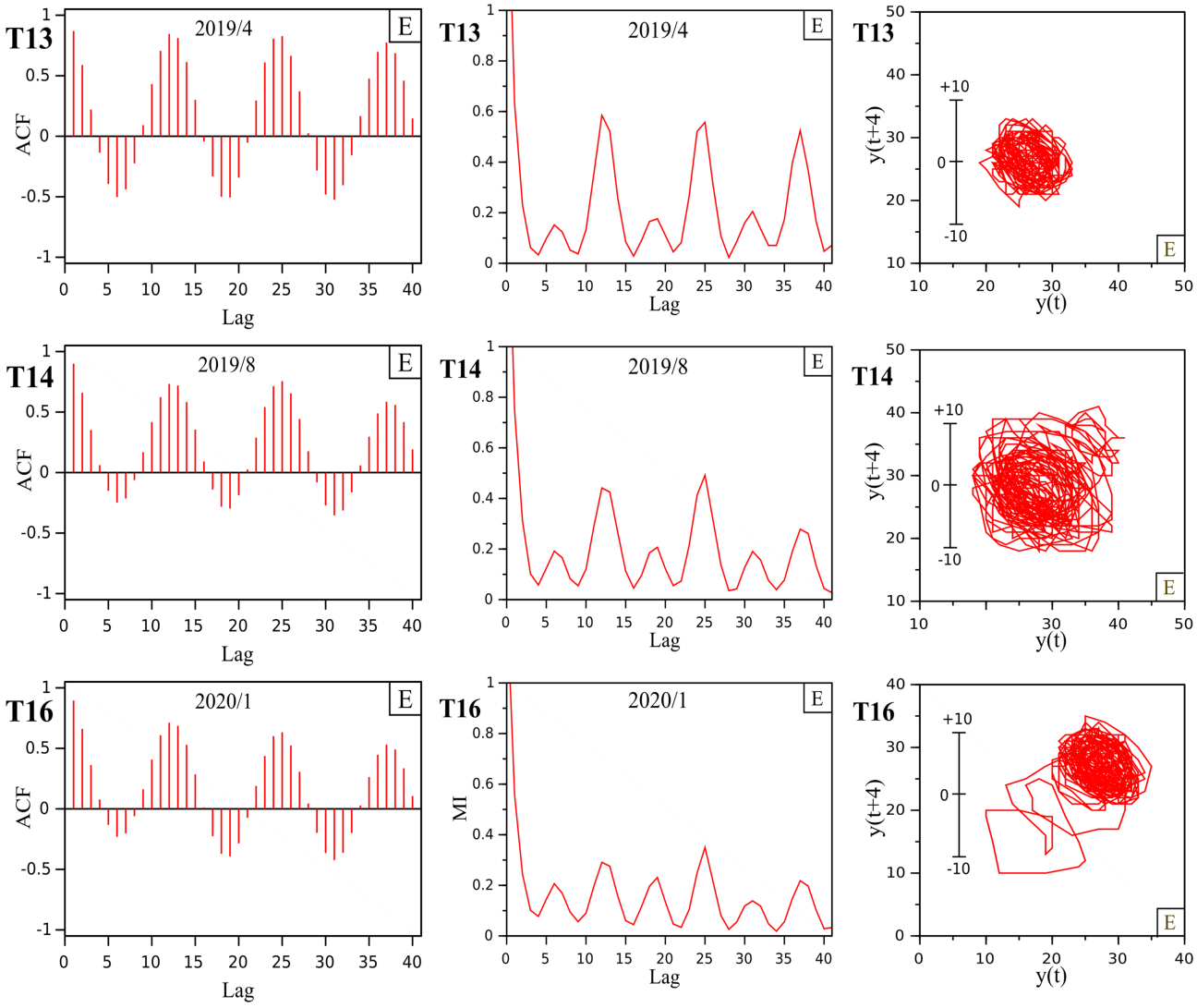

Figure 12. ACF, MI and the phase trajectories of tidal data named Type E.

Table 2. Frequency of each classified type in the time of Kuroshio's meandering.

Type A	Type B	Type C	Type D	Type E	Total
6	33	1	8	5	53

when the first bottom of MI is more than 0.05, the data are classified into Type E.

Phase trajectories of each classified type are also shown in from Figure 7 to Figure 12. Phase trajectories of Type A have a flattened shape and are stretched more than 20 cm in size. Phase trajectories of Type B are a round shape of 20 cm or so in size. Other types without Type A or Type B have a flattened and squared shape or take a random shape, and some orbit deviates.

Tidal data are classified into 5 types using ACF and MI in this paper. Table 2 shows the frequency of each classified type in terms of the 53 months data of Kuroshio's meandering. A lot of Type B occurs at the time of the meandering in Table 2 and the results are frequent next in order of Types A, D, E, and the ap-

pearance of Type C is rare. However, there are some data which are difficult to classify, because their character has diversity. The accuracy of classification can be generally regarded and calculated as a probabilistic model based on the mutual distance of classes and the dispersion of the data. The distance between classes depends on the number of classes. The number of classes required for the classification is not known currently. However, this paper divides the tidal data into five types. We think that the probability of misclassify between Type A and Type B is extremely low since the characteristics of ACF and MI are clearly different. In addition, we can see the perturbation by meteorological factors on a part of analysis results. With better data processing methods, we can improve the accuracy of classification. It would be worth studying the coefficient of each meteorological factor which affects the tidal data.

This classification is equivalent to a cluster analysis of machine learning without supervisor. Therefore, it is necessary to name each cluster. We study the meaning of each cluster using the mean of tide level difference or ADF test. The mean of tide level difference has been used as the clue which judged the sea conditions that had a relationship to the speed of the ocean current near the Kii Peninsula. The mean of tide level difference takes lower value because the speed of the ocean current is decreasing when Kuroshio is meandering and goes around Kii Peninsula. However, as for the flow speed is increasing when Kuroshio is approaching and flows near Kii Peninsula. On the contrary, the mean of tide level difference takes higher values.

Table 3 shows the classification results and the monthly mean of tidal data shown in Figure 5. Total time of Kuroshio's meandering is 55 months for 16 years from 2004 to 2020, and 53 months data can be classified. Figure 13 shows

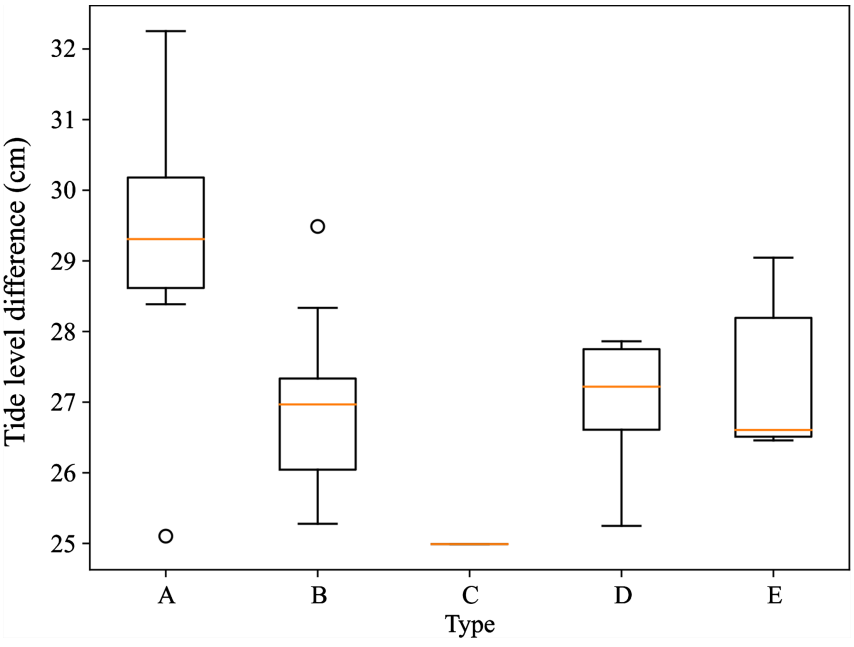

Figure 13. Box and whisker chart of the monthly mean of tide level difference for each classified type.

the box and whisker chart of the monthly mean of tide level difference for each type. Lower whisker shows the minimum and upper whisker is at the maximum. Orange line is at the medium and open circles show outliers.

Tidal data of Type A has an obviously high value compared with other types at the term of Kuroshio's meandering. The increasing of the mean tide level difference shows the approaching situations of Kuroshio Current. We think this phenomenon is the cause of the Kuroshio's non-meandering, transitions process from non-meandering to meandering or from meandering to non-meandering. As a result, we name an unstable state, non-steady state as Type A. On the contrary, the mean of tide level difference of Type C is the lowest, but we couldn't discuss it because Type C is observed only once during 53 months yet. The clear difference on the mean tidal data does not appear between Types B, D, and E in **Figure 13**.

Now that, we would like to give Type B the meaning in terms of the tidal motion using ADF test. Type B frequently occurs at the time of the Kuroshio's meandering in **Table 2**. According to the ADF test, the tidal motion is said a stationary process by rejecting the null hypothesis of a non-stationary process. **Table 4** shows the t-statistic and the p-value of ADF test. When the p-value is less than 5%, the null hypothesis is rejected and the tidal motion takes a stationary process. We can also compare the t-statistic to the critical value calculated by W. A. Fuller and the critical value is about −3.4 [27]. The stationary processes of total 41 times are seen during Kuroshio's meandering of 53 months in **Table 4**.

Figure 14 shows the p-values of every month from 2004 to 2005 and from 2017 to 2020. The p-values are low frequently when the Kuroshio flows meandering paths. In contrast, the p-values are a wide variety of value when the Kuroshio flows non-meandering paths. However, there are some exceptions. For example, the p-values of T1 and T6 in **Figure 14** are low and mean the stationary state but they are in the term of the non-meandering flow. These results show that the tidal movement changes to the non-stationary process when Kuroshio's paths change from the meandering flow to the non-meandering flow.

Figure 15 shows the box and whisker chart of the p-value of ADF test for each classified type, and **Figure 16** shows the box and whisker chart of the t-statistic of ADF test for that. Lower whisker shows the minimum and upper whisker is at the maximum. Orange line is at the medium and open circles show outliers. Broken line in **Figure 15** and **Figure 16** means the critical value of 5%, so at the 95 percent level the null hypothesis of a unit root will be rejected when p-value and t-statistic are lower than that. When the tide level data show Type B, the sea conditions and the tide are periodic and steady, and we can suppose that they are stable because the tidal data of Type B have the periodic characteristics as shown in **Figure 6(b)** and **Figure 9**. Type C is observed only once during 53 months in Kuroshio's meandering and shows stationary process. The tidal data of Type C have the irregular random characteristics in **Figure 6(c)** and **Figure 10** of T15. Therefore, Type C is considered the irregular random and stationary process. Interestingly, Type C at the time of the non-meandering in **Table 4** of

T6, and it has the irregular random property. These data are the stationary process and can be approved by using ADF test. Park *et al.* distinguished chaos system and a random walk using ADF test in addition to the new test that they

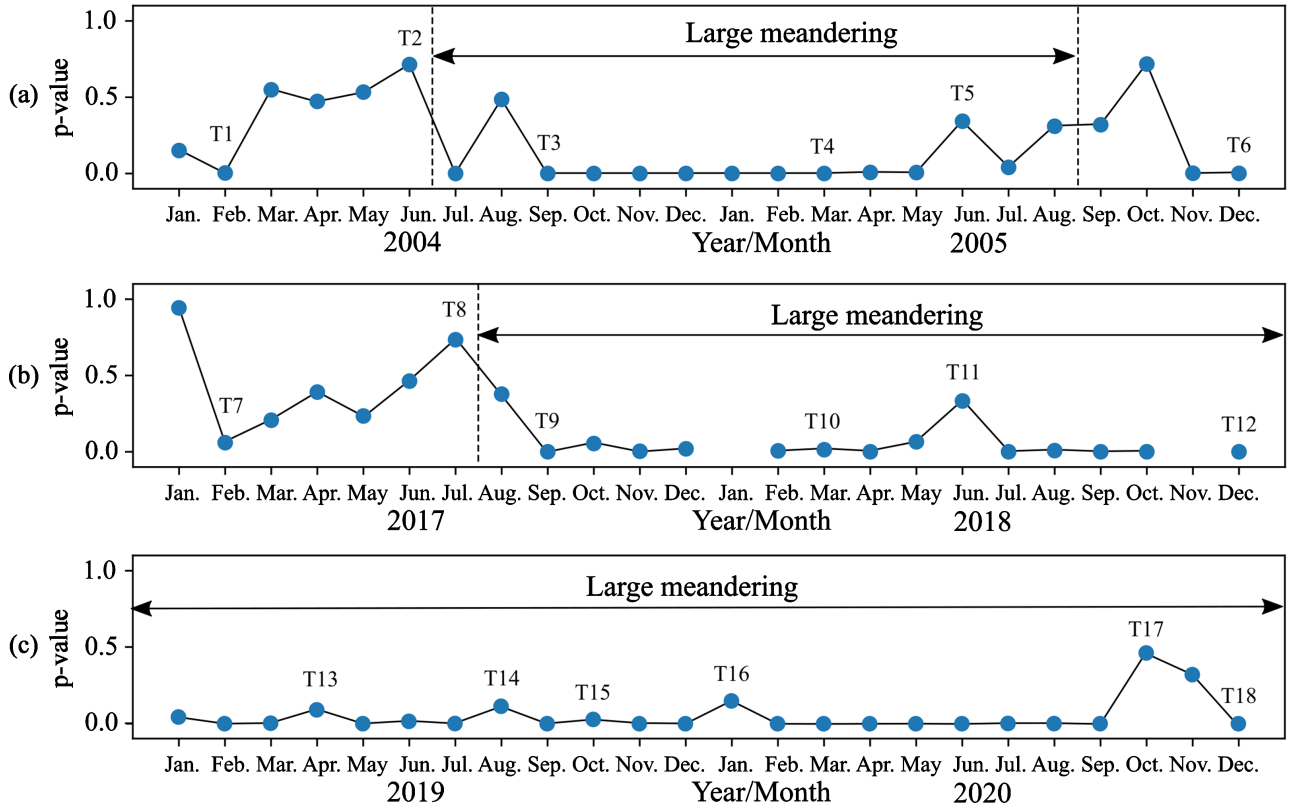

Figure 14. P-value of tidal data for each month in 2004, 2005 and from 2017 to 2020.

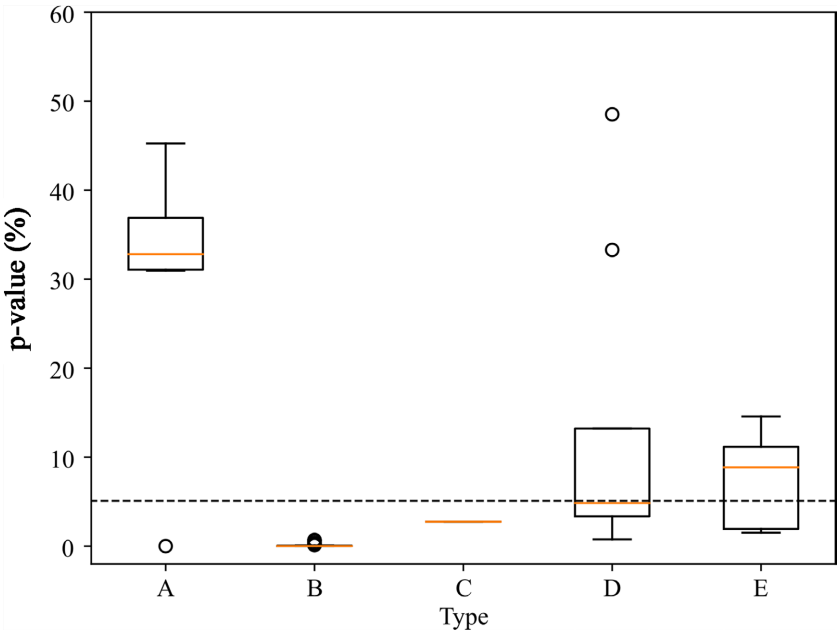

Figure 15. Box and whisker chart of the p-value of ADF test for each classified type. Broken line means the border of the critical p-value of 5%.

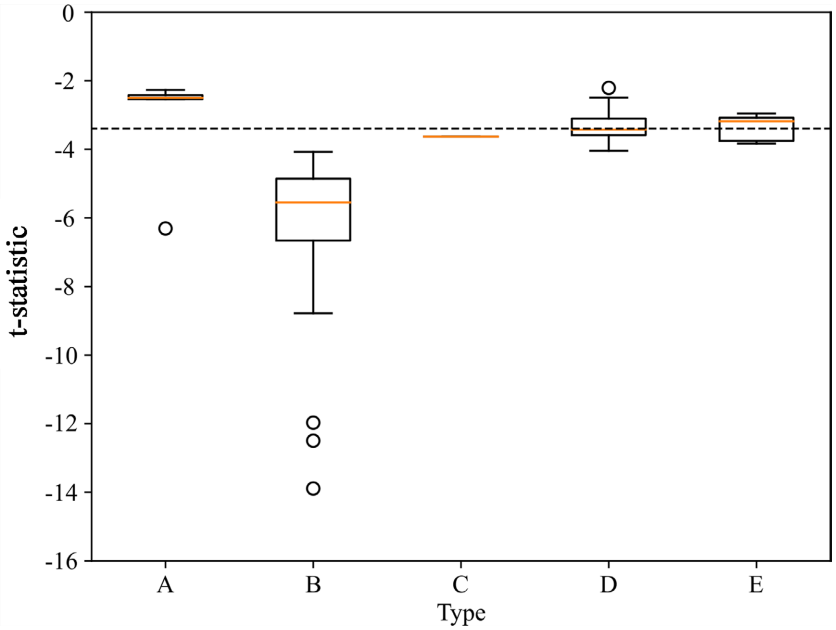

Figure 16. Box and whisker chart of the t-statistic of ADF test for each classified type. Broken line means the border of the t-statistic of 5% in p-value.

Table 3. The classification and monthly mean of tide level difference data (tidal data).

Month year	Type	Mean of tidal data (cm)	Month year	Type	Mean of tidal data (cm)	Month year	Type	Mean of tidal data (cm)
Jan. 2004	D	32.42	Jan. 2017	A	35.27	Jan. 2019	D	27.86
Feb. 2004	A	31.94	Feb. 2017	D	31.72	Feb. 2019	B	26.88
Mar. 2004	A	36.93	Mar. 2017	D	35.04	Mar. 2019	B	26.97
Apr. 2004	A	42.37	Apr. 2017	D	37.45	Apr. 2019	E	26.51
May 2004	D	42.69	May 2017	A	32.08	May 2019	B	26.86
Jun. 2004	A	38.84	Jun. 2017	A	32.49	Jun. 2019	E	26.46
Jul. 2004	A	25.10	Jul. 2017	A	44.21	Jul. 2019	B	26.69
Aug. 2004	D	25.25	Aug. 2017	A	30.46	Aug. 2019	E	28.19
Sep. 2004	B	25.56	Sep. 2017	B	28.29	Sep. 2019	B	27.12
Oct. 2004	B	26.05	Oct. 2017	D	27.54	Oct. 2019	C	24.99
Nov. 2004	B	25.97	Nov. 2017	B	29.49	Nov. 2019	B	27.41
Dec. 2004	B	25.95	Dec. 2017	E	29.05	Dec. 2019	B	26.96
Jan. 2005	B	25.81	Jan. 2018	*	*	Jan. 2020	E	26.61
Feb. 2005	B	25.28	Feb. 2018	B	28.33	Feb. 2020	B	26.76
Mar. 2005	B	25.48	Mar. 2018	D	26.71	Mar. 2020	B	26.67
Apr. 2005	B	26.02	Apr. 2018	B	27.09	Apr. 2020	B	26.58
May 2005	B	25.46	May 2018	D	27.79	May 2020	B	27.15
Jun. 2005	A	28.39	Jun. 2018	D	27.74	Jun. 2020	B	27.16

Continued

Jul. 2005	D	26.32	Jul. 2018	B	27.33	Jul. 2020	B	27.58
Aug. 2005	A	29.31	Aug. 2018	D	26.90	Aug. 2020	B	27.15
Sep. 2005	A	43.30	Sep. 2018	B	27.34	Sep. 2020	B	27.02
Oct. 2005	A	38.53	Oct. 2018	B	27.40	Oct. 2020	A	32.25
Nov. 2005	C	32.93	Nov. 2018	*	*	Nov. 2020	A	29.31
Dec. 2005	C	41.63	Dec. 2018	B	28.00	Dec. 2020	B	27.76

*Represents non-execution of the analysis because of some data loss.

Table 4. T-statistic and p-value of ADF test.

Month year	T-statistic	P-value (%)	Month year	T-statistic	P-value (%)	Month year	T-statistic	P-value (%)
Jan. 2004	−2.937	15.04	Jan. 2017	−0.999	94.42	Jan. 2019	−3.468	4.29
Feb. 2004	−4.279	0.34	Feb. 2017	−3.342	5.96	Feb. 2019	−5.001	0.02
Mar. 2004	−2.096	54.74	Mar. 2017	−2.774	20.68	Mar. 2019	−4.291	0.32
Apr. 2004	−2.231	47.25	Apr. 2017	−2.378	39.12	Apr. 2019	−3.179	8.86
May 2004	−2.122	53.36	May 2017	−2.704	23.45	May 2019	−4.922	0.03
Jun. 2004	−1.780	71.42	Jun. 2017	−2.248	46.31	Jun. 2019	−3.831	1.51
Jul. 2004	−6.308	0.00	Jul. 2017	−1.737	73.43	Jul. 2019	−4.591	0.11
Aug. 2004	−2.208	48.52	Aug. 2017	−2.404	37.77	Aug. 2019	−3.078	11.16
Sep. 2004	−6.248	0.00	Sep. 2017	−6.492	0.00	Sep. 2019	−4.914	0.03
Oct. 2004	−11.97	0.00	Oct. 2017	−3.381	5.40	Oct. 2019	−3.630	2.74
Nov. 2004	−6.746	0.00	Nov. 2017	−4.269	0.35	Nov. 2019	−12.50	0.00
Dec. 2004	−13.89	0.00	Dec. 2017	−3.750	1.93	Dec. 2019	−6.568	0.00
Jan. 2005	−6.437	0.00	Jan. 2018	*	*	Jan. 2020	−2.953	14.57
Feb. 2005	−5.599	0.00	Feb. 2018	−4.122	0.59	Feb. 2020	−5.417	0.00
Mar. 2005	−5.535	0.00	Mar. 2018	−3.868	1.34	Mar. 2020	−6.644	0.00
Apr. 2005	−4.072	0.69	Apr. 2018	−5.652	0.00	Apr. 2020	−5.142	0.01
May 2005	−4.101	0.63	May 2018	−3.306	6.52	May 2020	−6.707	0.00
Jun. 2005	−2.471	34.25	Jun. 2018	−2.490	33.29	Jun. 2020	−4.981	0.02
Jul. 2005	−3.493	4.02	Jul. 2018	−5.564	0.00	Jul. 2020	−4.488	0.16
Aug. 2005	−2.537	30.96	Aug. 2018	−4.043	0.76	Aug. 2020	−4.677	0.08
Sep. 2005	−2.517	31.94	Sep. 2018	−8.780	0.00	Sep. 2020	−5.036	0.02
Oct. 2005	−1.774	71.73	Oct. 2018	−7.616	0.00	Oct. 2020	−2.267	45.25
Nov. 2005	−4.448	0.18	Nov. 2018	*	*	Nov. 2020	−2.529	31.37
Dec. 2005	−4.712	0.07	Dec. 2018	−7.260	0.00	Dec. 2020	−12.39	0.00

The t-statistic to reject a null hypothesis is less than −3.399 at 5%. *Represents non-execution of ADF test because of some data loss.

suggested [28]. Therefore, we assume that Type C is a stationary random process. The correlation of between the Type C and the stationary process is important and should be studied more. The data of Type D and Type E are distributed in both stationary process and non-stationary process. It is difficult to give the naming of the Type D and Type E of the characteristics from the results of ADF test. As for Type A, the p-value and t-statistic are high and take the non-stationary process.

As we mentioned above, there are some correlations between the mean tide level differences. The correlation coefficient between the data of the mean tide level difference in Table 3 and the p-values in Table 4 is 0.492. We can call that it is the moderate correlation if the correlation coefficient between two data is higher than 0.4. In addition, the correlation coefficient between the data of the mean tide level difference and the t-statistics is 0.270; we can call it the weak correlation of Kuroshio meanders which need more attention when their distributions are skew. In other words, this relation between the mean tide level difference and ADF test is rather weak. The weak correlation makes us use the ADF test because we can have various analyses.

4. Conclusion

In this paper, we analyze tidal data of Kuroshio Current in two different periods which are from 2004 to 2005 and from 2017 to 2020. The tide level data which are observed at Kushimoto and Uragami in the southern part of Kii Peninsula are affected very much by Kuroshio Current. Using ACF, MI, and the phase trajectories, the classification of tide level difference enables us to discuss the periodical tidal motion and the randomness at the time of Kuroshio meandering. The ADF test is used for judging whether the data is either the stationary process or the non-stationary process. We can give some typical classifications the meaning by the mean tide level difference and ADF test. The increasing of the mean tide level difference expects the situations of Kuroshio's non-meandering, the transitions process from non-meandering to meandering or from meandering to non-meandering. On the other hand, when both the mean tide level difference and statistics of ADF test are low, the tidal motion is a periodic and stationary process. If so, we can assume that sea condition is in a steady and stable process. The ADF test is useful as the same as the mean tide level difference to analyze Kuroshio's data for studying the sea conditions.

Acknowledgements

We express our appreciation to JODC (J-DOSS) for supplying the tide level data on their website.

Conflicts of Interest

The author declares no conflicts of interest regarding the publication of this paper.

References

[1] Sawada, K. and Harada, N. (1998) Variability of the Path of the Kuroshio Ocean Current over the Past 25,000 Years. *Nature*, **392**, 592-595. https://doi.org/10.1038/33391

[2] Nagai, T., Hasegawa, D., Tsutsumi, E., *et al.* (2021) The Kuroshio Flowing over Seamounts and Associated Submesoscale Flows Drive 100-Km-Wide 100-1000-Fold Enhancement of Turbulence. *Communications Earth & Environment*, **2**, Article No. 170. https://doi.org/10.1038/s43247-021-00230-7

[3] Yamauchi, A., Kawamoto, K., Manda, A. and Li, J. (2018) Assessing the Impact of the Kuroshio Current on Vertical Cloud Structure Using CloudSat Data. *Atmospheric Chemistry and Physics*, **18**, 7657-7667. https://doi.org/10.5194/acp-18-7657-2018

[4] Sato, K., Manda, A., Moteki, Q., *et al.* (2016) Influence of the Kuroshio on Mesoscale Convective Systems in the Baiu Frontal Zone over the East China Sea. *American Meteorological Society*, **144**, 1017-1033. https://doi.org/10.1175/MWR-D-15-0139.1

[5] Sugimoto, S., Qiu, B. and Schneider, N. (2021) Local Atmospheric Response to the Kuroshio Large Meander Path in Summer and Its Remote Influence on the Climate of Japan. *Journal of Climate*, **34**, 3571-3589. https://doi.org/10.1175/JCLI-D-20-0387.1

[6] Holloway, G. (1999) Moments of Probable Seas: Statistical Dynamics of Planet Ocean. *Physica D*: *Nonlinear Phenomena*, **133**, 199-214. https://doi.org/10.1016/S0167-2789(99)00092-5

[7] Xu, Y., Ma, L., Sune, Y., Li, X., Wang, H. and Zhang, H. (2019) Spatial Variation of Demersal Fish Diversity and Distribution in the East China Sea: Impact of the Bottom Branches of the Kuroshio Current. *Journal of Sea Research*, **144**, 22-32. https://doi.org/10.1016/j.seares.2018.11.003

[8] Morioka, Y., Varlamov, S. and Miyazawa, Y. (2019) Role of Kuroshio Current in Fish Resource Variability off Southwest Japan. *Scientific Reports*, **9**, Article No. 17942. https://doi.org/10.1038/s41598-019-54432-3

[9] Imawaki, S., Uchida, H., Ichikawa, H., Fukasawa, M., Umatani, S. and ASUKA Group (2001) Satellite Altimeter Monitoring the Kuroshio Transport South of Japan. *Geophysical Research Letters*, **28**, 17-20. https://doi.org/10.1029/2000GL011796

[10] Taniguchi, N., Huang, C., Kaneko, A., Liu, C., Howe, B.M., Wang, Y., Yang, Y., Lin, J., Zhu, X. and Gohda, N. (2013) Measuring the Kuroshio Current with Ocean Acoustic Tomography. *The Journal of the Acoustical Society of America*, **134**, 3272-3281. https://doi.org/10.1121/1.4818842

[11] Kawabe, M. (1995) Variations of Current Path, Velocity, and Volume Transport of the Kuroshio in Relation with the Large Meander. *Journal of Physical Oceanography*, **25**, 3103-3117. https://doi.org/10.1175/1520-0485(1995)025<3103:VOCPVA>2.0.CO;2

[12] Japan Meteorological Agency Website (2019) Weather, Climate & Earthquake Information. https://www.jma.go.jp/jma/en/menu.html

[13] Nakano, H., Tsujino, H. and Sakamoto, K. (2012) Tracer Transport in Cold-Core Rings Pinched off from the Kuroshio Extension in an Eddy-Resolving Ocean General Circulation Model. *Journal of Geophysical Research*: *Oceans*, **118**, 5461-5488. https://doi.org/10.1002/jgrc.20375

[14] Kawabe, M. (1987) Spectral Properties of Sea Level and Time Scales of Kuroshio Path

Variations. *Journal of the Oceanographical Society of Japan*, **43**, 111-123. https://doi.org/10.1007/BF02111887

[15] Terachi, S. and Ogata, S. (2000) Characteristics of Tide Level Affected by Kuroshio. In: *Proceedings of the XVI IMEKO World Congress*, Vienna, 25-28 September 2000, 1-6. https://www.imeko.org/index.php/proceedings/3995-characteristics-of-tide-level-affected-by-kuroshio

[16] Nakamura, T., Maekawa, Y., Nakazato, K., Koike, T., Takeuchi, J. and Nagata, Y. (2012) Seasonal Variation of the Sea Level Difference between Kushimoto and Uragami Tide-Gauge Station. *La Mer*, **50**, 77-84. (In Japanese)

[17] Moriyasu, S. (1961) On the Difference in the Monthly Sea Level between Kushimoto and Uragami, Japan. *Journal of the Oceanographical Society of Japan*, **17**, 197-200. https://doi.org/10.5928/kaiyou1942.17.197

[18] Yoshida, J., Maeta, E., Nakano, H., Deguchi, H. and Nemoto, M. (2014) Statistical Analysis of the Variation of the Kuroshio Path, *Oceanography in Japan*, **23**, 171-196. (In Japanese) https://doi.org/10.5928/kaiyou.23.5_171

[19] J-DOSS: JODC Data On-Line Service System. Provided by the Japan Oceanographic Data Center (JODC). https://www.jodc.go.jp/service.htm

[20] Frison, T.W., Abarbanel, H.D.I., Earle, M.D., Schultz, J.R. and Scherer, W.D. (1999) Chaos and Predictability in Ocean Water Levels. *Journal of Geophysical Research: Oceans*, **104**, 7935-7951. https://doi.org/10.1029/1998JC900104

[21] Fraser, A.M. and Swinney, H.L. (1986) Independent Coordinates for Strange Attractors from Mutual Information. *Physical Review A*, **33**, 1134-1140. https://doi.org/10.1103/PhysRevA.33.1134

[22] Ni, Q., Zhai, X., Wang, G. and Marshall, D.P. (2020) Random Movement of Mesoscale Eddies in the Global Ocean. *Journal of Physical Oceanography*, **50**, 2341-2357. https://doi.org/10.1175/JPO-D-19-0192.1

[23] Prabhakaran, S. (2019) Augmented Dickey Fuller Test (ADF Test). https://www.machinelearningplus.com/time-series/augmented-dickey-fuller-test/

[24] Dubois, E. and Michaux, E. (2015) Unit Roots and Cointegration. Grocer: An Econometric Toolbox for Scilab. http://grocer.toolbox.free.fr/grocer.html

[25] Sheppard, K. (2021) Unit Root Testing, arch.unitroot.ADF. https://arch.readthedocs.io/en/latest/unitroot/generated/arch.unitroot.ADF.html

[26] Kirimoto, K. (2016) Time-Frequency and Nonlinear Analysis of Tidal Data Observed on the Kuroshio Path. *International Journal of Modern Nonlinear Theory and Application*, **5**, 147-159. https://doi.org/10.4236/ijmnta.2016.54015

[27] Fuller, W.A. (1976) Introduction to Statistical Time Series. John Wiley and Sons, New York.

[28] Park, J.Y. and Whang, Y.J. (2012) Random Walk or Chaos: A Formal Test on the Lyapunov Exponent. *Journal of Econometrics*, **169**, 61-74. https://doi.org/10.1016/j.jeconom.2012.01.012